

# Searching for New Physics in $b$ -hadron decays

Thomas Latham on behalf of the LHCb collaboration

Department of Physics, University of Warwick, Coventry, CV4 7AL, United Kingdom

DOI: <http://dx.doi.org/10.3204/DESY-PROC-2014-04/297>

Recent results from the realm of  $b$ -hadron physics are presented, with a focus on anomalous results and  $CP$  violation studies. Results are shown from the  $B$ -factories: *BABAR* and *Belle*; the Tevatron experiments: *CDF* and *D0*; and the LHC experiments: *ATLAS*, *CMS* and *LHCb*. Together these give some tantalising hints of cracks in the Standard Model.

## 1 Introduction

One of the primary goals of the field of flavour physics is to uncover evidence of physics beyond the Standard Model (SM) of particle physics — so called “New Physics”. This is achieved by looking for discrepancies between the SM predictions and experimental results in observables such as decay rates and  $CP$ -violating asymmetries. It is therefore essential to have good precision in both experiment and theory. The searches that can be performed using flavour observables are complementary to the searches for New Physics (NP) particles at the energy frontier. Indeed, they can potentially probe higher energy scales than those that are currently directly accessible. The study of  $b$ -hadrons and their decays provides an excellent laboratory in which to make such measurements. Such studies are a world-wide effort, with experiments in the USA, Europe and Japan all contributing. Some of latest results from these experimental collaborations will be presented here.

## 2 Measurements of $CP$ -violating phases

### 2.1 CKM angle $\gamma$

Of the three angles of the UT, the angle  $\gamma$  is the least well determined. Of particular importance is that the angle  $\gamma$  can be determined from purely tree-level processes. In addition, these determinations are theoretically extremely clean; the correspondence between the experimental measurements and the SM value of  $\gamma$  is accurate to the level of  $10^{-7}$  [1]. Such measurements are therefore a “standard candle” for the SM and can be compared with measurements from loop-dominated processes to look for discrepancies. Hence, it is very important to achieve the best possible experimental precision.

The two tree-level diagrams  $b \rightarrow c\bar{u}s$  and  $b \rightarrow u\bar{c}s$  have a relative weak phase of  $\gamma$ . For this phase to be measurable the two diagrams must interfere. This can happen in the decays  $B^+ \rightarrow \bar{D}^0 K^+$  and  $B^+ \rightarrow D^0 K^+$  if the  $D^0$  and  $\bar{D}^0$  decay to the same final state. The experimental method depends on the nature of the  $D$  decay. The most recent results from LHCb use the decays  $D \rightarrow K_s^0 \pi^+ \pi^-$  and  $K_s^0 K^+ K^-$ , and hence the so-called GGSZ method [2, 3]. The strong

phase difference between the  $D^0$  and  $\bar{D}^0$  decays can be determined as a function of the position in the Dalitz plot, either by using a model of the decay amplitudes, e.g. from *BABAR* [4], or via a model-independent approach that uses measurements of the phase difference in bins of the Dalitz plot provided by the *CLEO-c* experiment [5]. The *LHCb* collaboration have recent results using both of these approaches. The model-dependent analysis [6] uses the data sample collected in 2011, corresponding to an integrated luminosity of  $1 \text{ fb}^{-1}$ . The model-independent analysis [7], described here, uses the  $3 \text{ fb}^{-1}$  Run 1 dataset (from 2011 and 2012).

The model-independent nature of the method essentially reduces the analysis to counting the number of  $B^+$  and  $B^-$  signal events in each bin of the Dalitz plot. The binning scheme is symmetric about  $m_+^2 = m_-^2$ , the bins in one half are labelled  $+i$ , while the corresponding bin in the other half is labelled  $-i$ . The signal yields are related to the quantities of interest via

$$\begin{aligned} N_{\pm i}^+ &= h_{B^+} \left[ F_{\mp i} + (x_+^2 + y_+^2) F_{\pm i} + 2\sqrt{F_i F_{-i}}(x_+ c_{\pm i} - y_+ s_{\pm i}) \right], \\ N_{\pm i}^- &= h_{B^-} \left[ F_{\pm i} + (x_-^2 + y_-^2) F_{\mp i} + 2\sqrt{F_i F_{-i}}(x_- c_{\pm i} - y_- s_{\pm i}) \right], \end{aligned} \quad (1)$$

where  $F_i$  is the fraction of events in bin  $i$  in the flavour-specific  $D^0 \rightarrow K_s^0 \pi^+ \pi^-$  Dalitz plot (obtained from semileptonic  $B^+ \rightarrow \bar{D}^0 \mu^+ \nu_\mu$  data),  $h_{B^\pm}$  are normalisation factors,  $c_i$  and  $s_i$  are the cosine and sine of the strong phase difference in bin  $i$  measured by *CLEO-c*, and  $x_\pm \equiv r_B \cos(\delta_B \pm \gamma)$  and  $y_\pm \equiv r_B \sin(\delta_B \pm \gamma)$ , where  $r_B$  and  $\delta_B$  are the ratio of magnitudes and strong phase difference of the two  $B$  decay diagrams. A simultaneous fit to the  $B$  candidate invariant mass in each Dalitz-plot bin is used to determine  $x_\pm$  and  $y_\pm$ . Interpreting these results in terms of the physical parameters gives

$$r_B = 0.080_{-0.021}^{+0.019}, \quad \delta_B = (134_{-15}^{+14})^\circ, \quad \gamma = (62_{-14}^{+15})^\circ,$$

which constitutes the single most precise measurement of  $\gamma$ .

## 2.2 $B_s^0$ - $\bar{B}_s^0$ mixing phase

The neutral  $B$  mesons exhibit mixing between  $B$  and  $\bar{B}$  through a box diagram. Decays to  $CP$  eigenstates, which are accessible for both  $B$  and  $\bar{B}$ , therefore allow the mixing phase to be probed via interference between the direct decay process and decay after mixing. In the  $B_s^0$  system, the SM prediction for the mixing phase is small,  $\phi_s \approx (-0.0363 \pm 0.0016)$  rad, while many NP models enhance this value.

The decay mode  $B_s^0 \rightarrow J/\psi \phi$  is experimentally very clean. However, the vector-vector final state is an admixture of  $CP$  eigenstates. An angular analysis is required to disentangle the  $CP$ -odd and  $CP$ -even components. The signal model is then a sum of terms containing both angular and time dependence. It is necessary to determine the flavour of the signal  $B$  meson at production. This can be achieved by using either flavour-specific decays of the other  $b$ -hadron in the event or particles (such as charged kaons) associated with the hadronisation of the signal  $B$ . It is also necessary to account for the efficiency as a function of both the decay time and the angular variables, as well as the experimental resolution on the same quantities. The *ATLAS*, *CMS* and *LHCb* collaborations have all recently reported new or improved measurements of  $\phi_s$ , which are shown in Fig. 1. The *ATLAS* [8] and *CMS* [9] results use the decay  $B_s^0 \rightarrow J/\psi \phi$ , while *LHCb* have a combination of the channels  $B_s^0 \rightarrow J/\psi \pi^+ \pi^-$  and  $B_s^0 \rightarrow J/\psi K^+ K^-$  using  $1 \text{ fb}^{-1}$  of data [10], as well as an update of the  $B_s^0 \rightarrow J/\psi \pi^+ \pi^-$  channel using the  $3 \text{ fb}^{-1}$  data set [11]. This latest *LHCb* results constitutes the single most precise measurement of

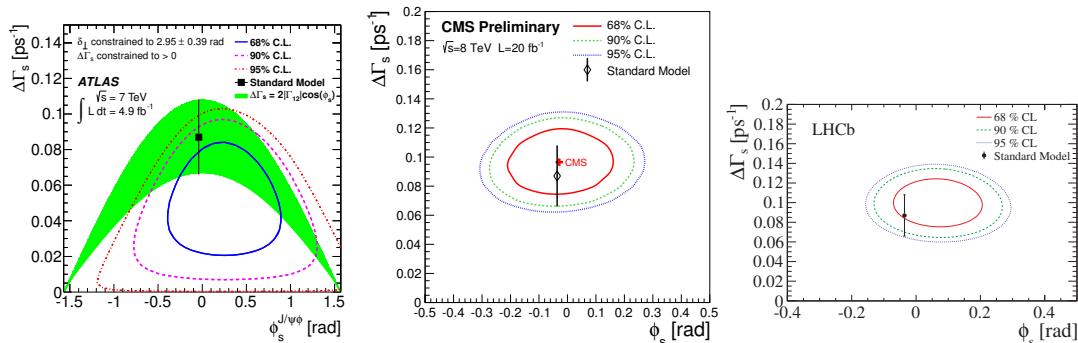


Figure 1: Results from (left) ATLAS, (middle) CMS, and (right) LHCb in the  $\Delta\Gamma_s$  vs  $\phi_s$  plane.

$\phi_s = (70 \pm 68 \pm 8)$  mrad. All of these results are consistent with the SM prediction. More precise measurements are needed to search for small deviations.

### 3 Semi-leptonic $B$ decays

Semi-leptonic decays of  $b$  hadrons can be used to measure the sides of the UT by determining the absolute values of the CKM elements  $V_{cb}$  and  $V_{ub}$ . There are some persistent puzzles in this area. Firstly, poor consistency between the values of  $V_{xb}$  measured in inclusive and exclusive decays, and secondly, the sum of the measured branching fractions of exclusive semi-leptonic  $B$  to charm decays falls well short of the well measured inclusive rate (inclusive – exclusive =  $(1.57 \pm 0.26)\%$ ). More precise measurements and measurements of extra decay channels are needed to either resolve these issues or to determine if they arise from NP contributions.

#### 3.1 Anomalies in $\bar{B} \rightarrow D^{(*)}\tau\bar{\nu}_\tau$

In addition to the above puzzles, the *BABAR* experiment sees a large deviation from the SM in semi-tauonic  $B$  to charm decays [12, 13]. Measurements are made of the ratio of branching fractions

$$R(D^{(*)}) = \frac{\text{BF}(\bar{B} \rightarrow D^{(*)}\tau\bar{\nu}_\tau)}{\text{BF}(\bar{B} \rightarrow D^{(*)}\ell\bar{\nu}_\ell)} = \frac{N_{\text{sig}}}{N_{\text{norm}}} \times \frac{\varepsilon_{\text{norm}}}{\varepsilon_{\text{sig}}}. \quad (2)$$

The results are  $R(D) = 0.440 \pm 0.072$  and  $R(D^*) = 0.332 \pm 0.030$ , which are  $2.0\sigma$  and  $2.7\sigma$  larger than the SM predictions  $0.297 \pm 0.017$  and  $0.252 \pm 0.003$ , respectively. The combined significance of the deviation is  $3.4\sigma$ . Including also the results from Belle [14, 15] increases the significance. Additionally, the *BABAR* results are incompatible (at the level of  $3.1\sigma$ ) with Type-II 2-Higgs-Doublet models of the possible charged Higgs contributions to these decays. The  $R(D)$  and  $R(D^*)$  results prefer different values of  $\tan\beta/m_{H^\pm}$  in these models. In addition, *BABAR* and Belle results of the branching fraction of  $B^- \rightarrow \tau^-\bar{\nu}_\tau$  prefer further different values of  $\tan\beta/m_{H^\pm}$ . The results can, however, be accommodated in more general 2-Higgs-Doublet models. The final results from the full Belle dataset are awaited with much anticipation.

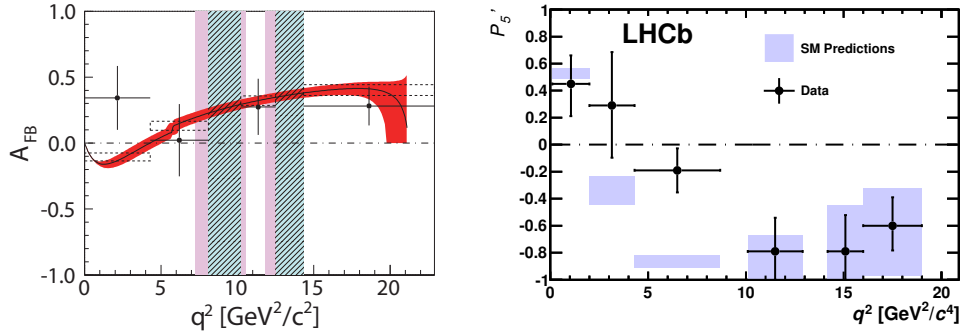


Figure 2: (left) Forward backward asymmetry as a function of  $q^2$  for inclusive  $B \rightarrow X_s \ell^+ \ell^-$ . The red band is the SM prediction. (right) Distribution of the  $P'_5$  angular observable for  $B^0 \rightarrow K^{*0} \mu^+ \mu^-$  decays.

### 3.2 Improved understanding of $\bar{B} \rightarrow D^{**} \ell \bar{\nu}_\ell$

The largest systematic uncertainty on the BABAR  $\bar{B} \rightarrow D^{(*)} \tau^- \bar{\nu}_\tau$  results is due to the modelling of backgrounds from  $B \rightarrow D^{**} \ell \nu_\ell$  decays. Many of these decays are not measured and this lack of knowledge could also be contributing to the “gap” between the inclusive and sum of exclusive branching fraction measurements mentioned earlier. Branching fractions of both charged and neutral  $B$  mesons decaying to  $D^{(*)} \pi^\pm \ell \nu_\ell$  and  $D^{(*)} \pi^+ \pi^- \ell \nu_\ell$  final states are measured by the BABAR experiment. For the latter class of decay, these are all first measurements, while those of the first type greatly improve their precision. The combined significance of the  $D \pi^+ \pi^- \ell \nu_\ell$  decays is  $5.1\sigma$ , while that of the  $D^* \pi^+ \pi^- \ell \nu_\ell$  decays is  $3.5\sigma$ . The inclusive–exclusive branching fraction gap is reduced from  $\sim 7\sigma$  to  $\sim 3\sigma$ . These new results should also help to improve the systematic uncertainties on future analyses of  $\bar{B} \rightarrow D^{(*)} \tau \bar{\nu}_\tau$ . A journal paper describing the analysis and its results is in preparation.

## 4 Rare decays

Decays of the type  $b \rightarrow s \ell^+ \ell^-$  proceed either via electroweak penguin or box diagrams. The Wilson coefficients  $C_7$ ,  $C_9$  and  $C_{10}$  encode the strength of the short-distance interactions. Many NP models predict additional contributions to the decay amplitudes at a similar level to the SM. Complementary information can be gained from branching fractions,  $CP$  asymmetries and angular moments, which are generally determined as a function of the 4-momentum transfer to the dimuon system,  $q^2$ .

The Belle collaboration have made the first measurements of the forward-backward asymmetry for inclusive  $B \rightarrow X_s \ell^+ \ell^-$  decays [16]. The analysis uses a sum of 10 exclusive final states: 3  $B^0$  decays to a charged kaon and 1–3 pions, and 7  $B^+$  decays to a charged kaon and 0–3 pions or a  $K_s^0$  and 1–3 pions. The data sample used comprises 772 million  $B\bar{B}$  pairs. The results are shown in Fig. 2 (left), where the red band is the SM prediction. Everything looks consistent with the SM at this level of precision, with the largest deviation being  $1.8\sigma$  in the first bin.

The LHCb collaboration have performed an analysis of angular observables that have been

optimised to reduce their dependence on form factors [17] in the decay  $B^0 \rightarrow K^{*0}\mu^+\mu^-$  [18]. The analysis uses the  $1\text{ fb}^{-1}$  data sample from 2011 and the results exhibit a large local deviation ( $3.7\sigma$ ) in one bin of the  $P'_5$  distribution, as can be seen in Fig. 2 (right). The probability to observe a fluctuation  $\geq 3.7\sigma$  in the 24 bins is 0.5%. The residual degree of dependence on form factors and hence the size of the theoretical uncertainties is a hot topic in the theory community. Improved determination of these as well as increased precision from the experimental side will help to determine if this is a genuine effect from NP contributions.

Including this result in global fits to the Wilson coefficients [19, 20, 21] indicates that it can be accommodated if the value of the  $C_9$  coefficient is reduced. If this is indeed the case then one would expect the branching fractions of decays such as  $B \rightarrow K^{(*)}\mu^+\mu^-$  and  $B_s^0 \rightarrow \phi\mu^+\mu^-$  to be lower than predicted. LHCb measurements of these quantities [22, 23, 24] are indeed lower than the predictions from both Lattice QCD [25, 26] and Light Cone Sum Rules [27, 28].

One possible explanation for a low value of  $C_9$  is contributions from a  $Z'$  particle, see for example Ref. [29]. Some NP models that include a  $Z'$  have preferred coupling to muons over electrons [30]. Due to destructive interferences this means that the branching fraction of  $B^+ \rightarrow K^+\mu^+\mu^-$  should be lower than that for  $B^+ \rightarrow K^+e^+e^-$ . LHCb also has results for this ratio of branching fraction using the full Run 1 data sample [31]

$$R_K = \frac{\text{BF}(B^+ \rightarrow K^+\mu^+\mu^-)}{\text{BF}(B^+ \rightarrow e^+e^-)} = 0.745_{-0.074}^{+0.090} \pm 0.036, \quad (3)$$

which deviates from the SM prediction of unity by  $2.6\sigma$ .

It would seem therefore that there is a reasonably consistent picture. However, there is much still to be understood, such as the importance of  $c\bar{c}$  resonances at high  $q^2$  [32, 33]. It is important to update all measurements to the full Run 1 data sample and to include additional decay modes, such as  $\Lambda_b \rightarrow \Lambda\mu^+\mu^-$  and  $B^+ \rightarrow K^+\pi^+\pi^-\ell^+\ell^-$ , to further increase the sensitivity.

## 5 Dimuon charge asymmetry

Measurements of the dimuon charge asymmetry are sensitive to possible  $CP$  violation in the mixing of the neutral  $B$  mesons, which would imply  $\Gamma(B \rightarrow \bar{B} \rightarrow \mu^- X) \neq \Gamma(\bar{B} \rightarrow B \rightarrow \mu^+ X)$ . The D0 experiment measures the inclusive dimuon asymmetry

$$A_{sl} = \frac{N(\mu^+\mu^+) - N(\mu^-\mu^-)}{N(\mu^+\mu^+) + N(\mu^-\mu^-)}, \quad (4)$$

which is related to both the semi-leptonic charge asymmetries of  $B^0$  and  $B_s^0$  mesons.

Corrections for backgrounds have been applied (the single muon asymmetry is used to help reduce systematic uncertainties), as well as those for  $CP$  violation that occurs in the interference between mixing and decay. After this, the result obtained by D0 [34] is  $A_{sl} = (-0.496 \pm 0.153 \pm 0.072)\%$ , which differs from the SM prediction,  $A_{sl}^{\text{SM}} = (-0.023 \pm 0.004)\%$ , at the level of  $2.8\sigma$ . Comparing separately each bin of the impact parameter distribution with the SM, the level of disagreement rises to  $3.6\sigma$ .

The interpretation of the result in terms of the individual semi-leptonic asymmetries depends strongly on the assumed value of  $\Delta\Gamma_d/\Gamma_d$ , the discrepancy with the SM varying between  $1.9\sigma$  and  $3.6\sigma$ . This highlights the importance of improved measurements of  $\Delta\Gamma_d/\Gamma_d$ . Indeed, a recent LHCb result [35] based on  $1\text{ fb}^{-1}$  of data and using the decay modes  $B^0 \rightarrow J/\psi K^{(*)0}$  gives a value  $-0.044 \pm 0.025 \pm 0.011$ , which is becoming competitive with the  $B$ -factory results.

## 6 Direct $CP$ violation in charmless three-body $B$ decays

In general,  $CP$  asymmetries can arise when there is more than one contributing amplitude to a decay and where those amplitudes have both different weak and strong phases. In charmless  $B^+$  decays there are contributing tree and loop diagrams, which have similar magnitudes and a relative weak phase of  $\gamma$ . In three-body decays, the strong phase difference could arise from an intrinsic difference in the two decay diagrams, from rescattering or from interference between intermediate resonances in the Dalitz plot.

### 6.1 Large $CP$ violation in $B^+ \rightarrow h^+h^+h^-$

The LHCb experiment has performed an analysis of  $CP$  violation in the phase-space of three-body charmless decays of  $B^+$  mesons to  $h^+h^+h^-$  final states ( $h = K/\pi$ ) [36]. The measured raw asymmetries are corrected for the effects of production, detection and matter-interaction asymmetries using data control modes. The inclusive asymmetries for each mode are determined to be between 2 – 13% in magnitude and positive (negative) for  $B^\pm \rightarrow K^\pm\pi^+\pi^-$  and  $\pi^\pm\pi^+\pi^-$  ( $B^\pm \rightarrow K^\pm K^+K^-$  and  $\pi^\pm K^+K^-$ ) decays. The local asymmetries in regions of the phase space are much more pronounced. Figure 3 shows the raw asymmetry as a function of the position in the Dalitz plot for the decays to  $K^\pm K^+K^-$  and  $K^\pm\pi^+\pi^-$ . There are regions of very large positive (negative) asymmetry at low values of the  $\pi^+\pi^-$  ( $K^+K^-$ ) invariant mass. A similar pattern is seen for the other two decay modes.

The larger data sample than the previous analyses [37, 38] allows a more detailed examination of the variation of the asymmetries in the phase space. Figure 4 shows the  $m_{\pi^+\pi^-}$  dependence of the difference between the  $B^-$  and  $B^+$  signal yields in the  $B^\pm \rightarrow \pi^\pm\pi^+\pi^-$  decay. The distributions are shown separately for the two regions  $\cos\theta > 0$  and  $\cos\theta < 0$ , where  $\theta$  is the angle between the like-sign pions in the  $\pi^+\pi^-$  rest frame. The most striking features are the change in sign of the asymmetry on either side of the  $\rho(770)$  resonance pole and that the sign is opposite for the two regions of  $\cos\theta$ . This indicates that the interference between the  $\rho(770)$  and an underlying  $S$ -wave component is playing a significant role in generating the  $CP$  asymmetry. In addition, it is possible that  $\pi\pi \leftrightarrow KK$  rescattering is contributing in the region between 1.2 and 1.5  $\text{GeV}/c^2$ . Amplitude analyses of these decays will be required to fully understand the origin of these very large asymmetries.

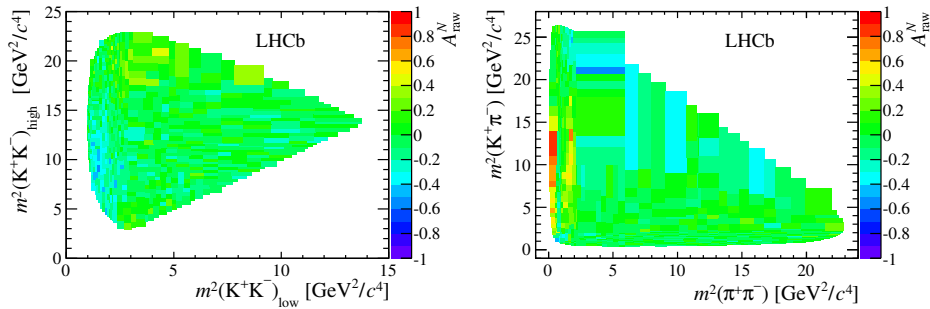


Figure 3: Raw asymmetries as a function of the DP position for  $B^\pm$  decays to (left)  $K^\pm K^+K^-$ , and (right)  $K^\pm\pi^+\pi^-$  final states.

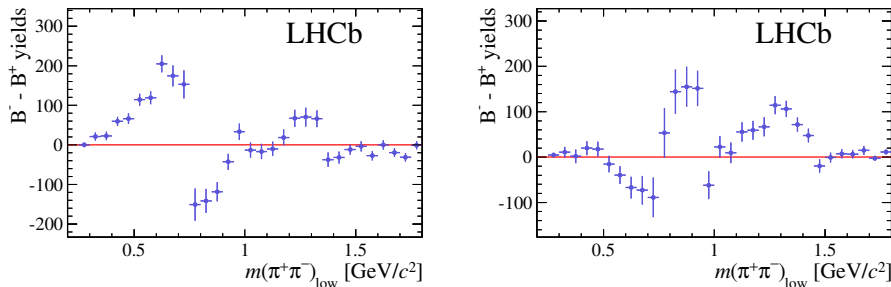


Figure 4: Difference of the  $B^-$  and  $B^+$  signal yields as a function of the  $\pi^+\pi^-$  invariant mass in the  $B^\pm \rightarrow \pi^\pm\pi^+\pi^-$  decay. The yields have been background-subtracted and efficiency-corrected.

## 6.2 Amplitude analysis of $B^+ \rightarrow K_S^0\pi^+\pi^0$

The *BABAR* experiment has recently performed an amplitude analysis of the decay  $B^+ \rightarrow K_S^0\pi^+\pi^0$ . In addition to providing measurements of the branching fractions and  $CP$  asymmetries of the various intermediate states, a Dalitz-plot analysis allows the determination of their relative phases. Of particular interest are the relative phases of the two  $K^*\pi$  components, which can be used to determine the CKM angle  $\gamma$  [39, 40].

A maximum likelihood fit is performed to separate signal from background and to determine the signal Dalitz-plot amplitudes. The fitted signal yield is  $1014 \pm 63$ , where the uncertainty is statistical only. The signal Dalitz-plot model follows the isobar model formalism, where the total amplitude is formed from the sum of the amplitudes for the various intermediate states. The complex coefficient for each contributing amplitude is determined from the fit. The branching fractions,  $CP$  asymmetries and relative phases are derived from these fitted coefficients. The signal model includes contributions from both the charged and neutral  $K^*(892)$  resonances and the corresponding  $K\pi$  S-wave as well as the  $\rho(770)^+$  resonance.

The  $CP$  asymmetry of  $B^+ \rightarrow K^*(892)^+\pi^0$  has a very large, negative central value ( $-52\%$ ) and is found to have a significance of  $3.4\sigma$ , corresponding to first evidence of  $CP$  violation in this decay. The projection of the fit onto the  $K_S^0\pi^+$  invariant mass can be seen in Figure 5, separated by the charge of the  $B$  candidate, where the asymmetry in the  $K^*(892)^+$  region can be clearly seen. A journal paper describing the analysis and its results is in preparation.

## 7 Conclusion

With increasingly precise and sophisticated measurements, some anomalies have started to appear within the realm of  $b$ -hadron physics. Whether these are true hints of contributions from physics beyond the Standard Model will only become apparent with improved measurements and theoretical understanding. The coming years will provide better experimental precision as the LHC Run 1 data is fully exploited and the samples from Run 2 are collected and analysed. With the start of the Belle II experiment and the upgrade of the LHCb experiment both expected within the next few years, we look forward to the unprecedented precision that these complementary experiments will offer across the whole range of  $b$ -hadron physics.

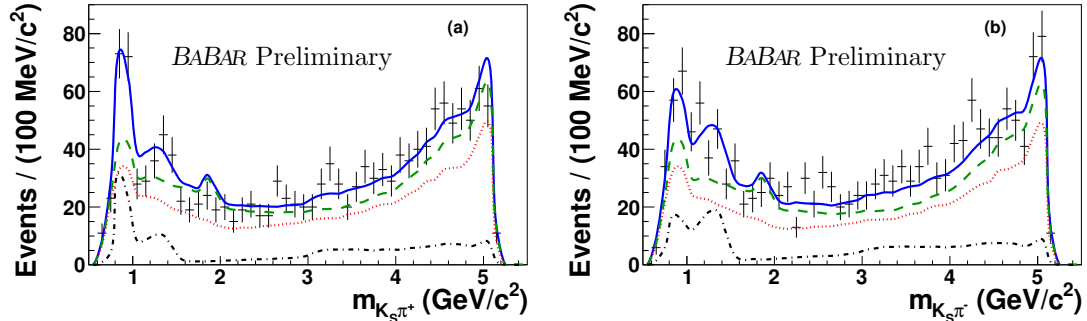


Figure 5: Data distributions of  $m_{K_S^0 \pi^+}$  and the corresponding fit projections for (a)  $B^+$ , and (b)  $B^-$  candidates. Points with error bars are the data, the solid (blue) lines are the total fit result, the dashed (green) lines are the total background contribution, and the dotted (red) lines are the  $q\bar{q}$  component. The dash-dotted lines represent the signal contribution.

## Acknowledgments

Work supported by the European Research Council under FP7 and by the Science and Technology Facilities Council.

## References

- [1] J. Brod and J. Zupan, JHEP **1401** (2014) 051.
- [2] A. Bondar, Proceedings of BINP special analysis meeting on Dalitz analysis, 24-26 Sept, 2002. Unpublished.
- [3] A. Giri, Y. Grossman, A. Soffer and J. Zupan, Phys. Rev. D **68** (2003) 054018.
- [4] P. del Amo Sanchez *et al.* [BaBar Collaboration], Phys. Rev. Lett. **105** (2010) 081803.
- [5] J. Libby *et al.* [CLEO Collaboration], Phys. Rev. D **82** (2010) 112006.
- [6] R. Aaij *et al.* [LHCb Collaboration], Nucl. Phys. B **888** (2014) 169.
- [7] R. Aaij *et al.* [LHCb Collaboration], Submitted to JHEP, arXiv:1408.2748 [hep-ex].
- [8] G. Aad *et al.* [ATLAS Collaboration], Phys. Rev. D **90** (2014) 052007.
- [9] CMS Collaboration, CMS-PAS-BPH-13-012 (2014).
- [10] R. Aaij *et al.* [LHCb Collaboration], Phys. Rev. D **87** (2013) 112010.
- [11] R. Aaij *et al.* [LHCb Collaboration], Phys. Lett. B **736** (2014) 186.
- [12] J. P. Lees *et al.* [BaBar Collaboration], Phys. Rev. Lett. **109** (2012) 101802.
- [13] J. P. Lees *et al.* [The BaBar Collaboration], Phys. Rev. D **88** (2013) 072012.
- [14] I. Adachi *et al.* [Belle Collaboration], arXiv:0910.4301 [hep-ex].
- [15] A. Bozek *et al.* [Belle Collaboration], Phys. Rev. D **82** (2010) 072005.
- [16] Y. Sato *et al.* [Belle Collaboration], arXiv:1402.7134 [hep-ex].
- [17] J. Matias, F. Mescia, M. Ramon and J. Virto, JHEP **1204** (2012) 104.
- [18] R. Aaij *et al.* [LHCb Collaboration], Phys. Rev. Lett. **111** (2013) 191801.
- [19] S. Descotes-Genon, J. Matias and J. Virto, Phys. Rev. D **88** (2013) 074002.
- [20] W. Altmannshofer and D. M. Straub, Eur. Phys. J. C **73** (2013) 2646.

- [21] F. Beaujean, C. Bobeth and D. van Dyk, *Eur. Phys. J. C* **74** (2014) 2897.
- [22] R. Aaij *et al.* [LHCb Collaboration], *JHEP* **1307** (2013) 084.
- [23] R. Aaij *et al.* [LHCb Collaboration], *JHEP* **1308** (2013) 131.
- [24] R. Aaij *et al.* [LHCb Collaboration], *JHEP* **1406** (2014) 133.
- [25] C. M. Bouchard, G. P. Lepage, C. J. Monahan, H. Na and J. Shigemitsu, arXiv:1310.3207 [hep-lat].
- [26] R. R. Horgan, Z. Liu, S. Meinel and M. Wingate, *Phys. Rev. Lett.* **112** (2014) 212003.
- [27] C. Bobeth, G. Hiller and D. van Dyk, *JHEP* **1107** (2011) 067.
- [28] C. Bobeth, G. Hiller, D. van Dyk and C. Wacker, *JHEP* **1201** (2012) 107.
- [29] R. Gauld, F. Goertz and U. Haisch, *JHEP* **1401** (2014) 069.
- [30] W. Altmannshofer, S. Gori, M. Pospelov and I. Yavin, *Phys. Rev. D* **89** (2014) 095033.
- [31] R. Aaij *et al.* [LHCb Collaboration], *Phys. Rev. Lett.* **113** (2014) 151601.
- [32] R. Aaij *et al.* [LHCb Collaboration], *Phys. Rev. Lett.* **111** (2013) 112003
- [33] J. Lyon and R. Zwicky, arXiv:1406.0566 [hep-ph].
- [34] V. M. Abazov *et al.* [D0 Collaboration], *Phys. Rev. D* **89** (2014) 012002.
- [35] R. Aaij *et al.* [LHCb Collaboration], *JHEP* **1404** (2014) 114.
- [36] R. Aaij *et al.* [LHCb Collaboration], Submitted to *Phys. Rev. D*, arXiv:1408.5373 [hep-ex].
- [37] R. Aaij *et al.* [LHCb Collaboration], *Phys. Rev. Lett.* **111** (2013) 101801.
- [38] R. Aaij *et al.* [LHCb Collaboration], *Phys. Rev. Lett.* **112** (2014) 011801.
- [39] M. Ciuchini, M. Pierini and L. Silvestrini, *Phys. Rev. D* **74** (2006) 051301.
- [40] M. Gronau, D. Pirjol, A. Soni and J. Zupan, *Phys. Rev. D* **75** (2007) 014002.